

3-1 A2

VLF RAY FOCUSING AND RADIATION PATTERNS OF ELECTRIC AND MAGNETIC DIPOLES IN A MULTICOMPONENT MAGNETOPLASMA

by
T. H. C. Wang* and T. F. Dell*

*Radio Physics Laboratory, Stanford Research Institute, Menlo Park, California 94025, U.S.A.

*Radioscience Laboratory, Stanford University, Stanford, California 94305, U.S.A.

In evaluating recent ideas concerning the operation of satellite-based VLF transmitters in the magnetosphere, it is important to know the VLF radiation pattern from an antenna in a magnetoplasma. Although the far fields from a radiating source in a magnetoplasma can be estimated from saddle point evaluations,^{1,2} for the VLF range the number of contributing saddle points depends strongly on the point of observation, and higher order saddle points frequently appear.^{2,3} These facts make the study of VLF antenna radiation patterns considerably complicated if one uses the time averaged pointing vector from the far fields. In the present paper, we shall employ an alternative method, noted earlier by Sturza,³ to study the details of the VLF radiation pattern of both electric and magnetic loops in a cold, collisionless, multicomponent magnetoplasma. In brief, this method is described as follows: The total time-averaged complex power radiated from a time harmonic current is formally given in terms of an integral in its Fourier spectrum:

$$P = -\frac{1}{2} \int \vec{K}(-\vec{k}) \cdot \vec{J}(\vec{k}) d\vec{k}. \quad (1)$$

(The full expression of $\vec{K}(-\vec{k})$ due to a Fourier transformed current $\vec{J}(\vec{k})$ is given elsewhere.³) To extract real radiated power, P_r , from (1), one can employ a contour integration in $|\vec{k}|$, yielding:

$$P_r = \int_{\theta, \phi} f(\theta, \phi) \sin\theta \, d\theta \, d\phi \quad (2)$$

where θ and ϕ are the spherical polar angle and the azimuthal angle for wave number vector $\vec{k} = \vec{k}/\beta$ ($\beta = \omega/c$, wave number in free space). For the case of the lossless system considered, (2) is a representation of total real radiated power summed up from all the rays in the wave normal space. In terms of observation coordinates, one may use a set of relations $\theta = \theta(\gamma, \varphi)$ and $\phi = \phi(\gamma, \varphi)$, where γ, φ is the polar angle and the azimuthal angle in the observation space, and rewrite (2) as:

$$P_r = \int_{\gamma, \varphi} \frac{\tilde{Y}(\gamma, \varphi)}{\sin\gamma} \frac{\partial(\theta, \phi)}{\partial(\gamma, \varphi)} \sin\gamma \, d\gamma \, d\varphi \quad (3)$$

where $\tilde{Y}(\gamma, \varphi)$ stands for $f(\theta, \phi) \sin\theta$, with θ and ϕ expressed in terms of γ and φ , and where $\partial(\theta, \phi)/\partial(\gamma, \varphi)$ is the Jacobian of the transformation. From (3), the mean power flux per unit solid angle (radiation pattern) in the observation coordinates is clearly:

$$\Gamma(\gamma, \varphi) = \frac{\tilde{Y}(\gamma, \varphi)}{\sin\gamma} \frac{\partial(\theta, \phi)}{\partial(\gamma, \varphi)} \quad (4)$$

where $\theta = \theta(\gamma, \varphi)$ and $\phi = \phi(\gamma, \varphi)$. For the case of a cold magnetoplasma, if the polar axis is chosen to be parallel to the static magnetic field \vec{H}_0 , the refractive indices of the two characteristic modes $n_{\pm}(\theta)$ are independent of ϕ .⁴ As a result of this particular property of $n_{\pm}(\theta)$, the subsidiary conditions become $\theta = \theta(\gamma)$ and $\phi = \varphi$, and $\partial(\theta, \phi)/\partial(\gamma, \varphi) = |\partial\theta/\partial\gamma|$. To calculate the relation $\theta = \theta(\gamma)$, one can use the saddle point relation:

$$\frac{\partial}{\partial\theta} [n(\theta)\cos(\gamma \pm \theta)] = 0, \quad \frac{\partial^2}{\partial\theta^2} [n(\theta)\cos(\gamma \pm \theta)] \neq 0. \quad (5)$$

A manipulation of (5) yields:

$$\gamma = \theta - \arctan(n'/n), \quad n' = dn(\theta)/d\theta \quad (6a)$$

$$\frac{\partial\theta}{\partial\gamma} = \frac{n^2 + (n')^2}{n^2 + 2(n')^2 - nn''}, \quad n'' = dn'/d\theta. \quad (6b)$$

In general, (6) together with $\varphi = \phi$ can be used in (4) to construct the radiation pattern for a given source in the plasma. However, if the refractive index surface (at a given frequency) possesses inflection points at some $\theta = \theta_m$, then here $\partial\theta/\partial\gamma = \infty$, and (3) and (4) are no longer valid. In this case, in order to continue the radiation pattern through the inflection points, it is necessary to supply additional relations, which leads to the introduction

of "focusing factor" outlined below.

From Eqs. (14d), (16), and (17) of Arbel and Felsen² we derive the following condition on the derivative of $\theta(\theta)$ ($\theta(\theta) = n(\theta)\cos(\gamma \pm \theta)$) for which (6), the single saddle-point relation, is a valid approximation:

$$\left[\frac{\partial^2 \theta(\theta)}{\partial\theta^2} \right]^2 \gg \left(\frac{2}{8r} \right)^{2/3} \left[\frac{\partial^3 \theta(\theta)}{\partial\theta^3} \right]^{4/3} \quad (7)$$

where r is a radial distance. Eqs. (6a) and (7) can be used to define a range of wave normal angles for which the single saddle point technique is valid. It can be shown that as $\theta \rightarrow \theta_m$, the right-hand side of (7) will eventually become greater than the left. When this occurs a second order saddle point evaluation is appropriate. Since by assumption the quantity $8r$ is a large number, it is clear that (7) must be satisfied for angles within a few degrees of θ_m . We now define implicitly two angles of "closest approach" (θ_r) to θ_m by means of (6a) and the relation

$$\frac{\partial^2 \theta}{\partial\theta^2} = \pm \left(\frac{20}{8r} \right)^{1/3} \left[\frac{\partial^3 \theta}{\partial\theta^3} \right]^{2/3}. \quad (8)$$

The two angles of interest in (8) are the two real roots which minimize the quantity $|\theta_r - \theta_m|$. By expanding the left-hand side of (8) in a Taylor series about θ_m , these two angles can be found approximately:

$$\theta_r - \theta_m \approx \pm \left(\frac{20}{8r} \right)^{1/3} \left[\frac{\partial^3 \theta}{\partial\theta^3} \right]_{\theta=\theta_m}^{-1/3}. \quad (9)$$

By the use of (6a) and (7), the wave normal angles θ_m and θ_r can be associated with the angles γ_m and γ_r in the observation coordinates. The ratio of the power flux flowing in the direction γ_m to that flowing in the direction γ_r , which we shall call the "focusing factor," can be deduced from Eqs. (10) and (18) of Arbel and Felsen:²

$$F = \left[\frac{\Gamma(\gamma_r)}{\Gamma(\gamma_m)} \right]^2 \left| \frac{\partial\theta}{\partial\gamma} \right|_{\gamma_r}^{1/3} \left| \frac{\partial\theta}{\partial\gamma} \right|_{\gamma_m}^{-1/3} \quad (10)$$

where $\theta'' = \partial^2\theta/\partial\theta^2$, $\theta''' = \partial^3\theta/\partial\theta^3$, and where all quantities are to be evaluated at $\theta = \theta_r$.

The radiation pattern of an arbitrary source in the magnetoplasma can now be found in the following way. First we define a distance from the source to the observation point. Eqs. (4) and (6) can be used for all angles, θ , which satisfy (7), including θ_m . The value of the power flux at γ_m is then obtained by multiplying the power flux at γ_r by the "focusing factor," F . Points lying in the narrow interval between γ_r and γ_m can be approximated by fitting a smooth curve between the known values of the power flux at γ_r and γ_m , with the maximum of the curve at γ_m .

Using the above developments together with the explicit expressions for the real radiated power, P_r , for either an electric dipole or a magnetic loop, given in our earlier papers,⁴⁻⁶ (4) is now written explicitly for the signal frequencies between the electron gyrofrequency f_{ge} and the proton gyrofrequency,

$$\Gamma_d(\gamma, \varphi) = C_d \Gamma_e(\gamma) \cos^2 \theta_0 + \Gamma_m(\gamma, \varphi) \sin^2 \theta_0 \frac{\sin\theta}{\sin\gamma} \left| \frac{\partial\theta}{\partial\gamma} \right| \quad (11a)$$

$$\Gamma_L(\gamma, \varphi) = C_L L_m(\gamma) \cos^2 \theta_0 + L_e(\gamma, \varphi) \sin^2 \theta_0 \frac{\sin\theta}{\sin\gamma} \left| \frac{\partial\theta}{\partial\gamma} \right| \quad (11b)$$

where Γ_d is the infinitesimal unit electric dipole radiation pattern, Γ_L is the infinitesimal unit magnetic dipole radiation pattern, C_d is the angle between the dipole axis and the static magnetic field,

$$C_d = \frac{\beta C^2 \omega}{32\pi^2 c}, \quad C_L = \frac{\beta C^2 \omega}{32\pi^2}, \quad C = 3 \times 10^8 \text{ m/sec and}$$

$$\Gamma_e(\gamma) = \frac{n^3 (n^2 - \epsilon_1)(n^2 - \epsilon_2)}{q(\theta)(n^2 - \epsilon_0)} \cos^2 \theta_0$$

$$\Gamma_1(\nu, \varphi) = \frac{n^3(n^2 - \epsilon_0)}{q(\theta)} \left[\cos^2 \varphi + \frac{\epsilon_d^2}{(n^2 - \epsilon_{-1})(n^2 - \epsilon_{-1})} \right] \sin^2 \theta \quad (12)$$

$$L_1(\nu) = \frac{\epsilon_d^2 n^5 (n^2 - \epsilon_0)}{q(\theta)(n^2 - \epsilon_{-1})(n^2 - \epsilon_{-1})} \sin^2 \theta$$

$$L_2(\nu, \varphi) = \left[\frac{n^5 (\epsilon_0 - \epsilon_{-1})(\epsilon_0 - \epsilon_{-1})}{q(\theta)(n^2 - \epsilon_0)} \sin^2 \varphi + L_1(\nu) \right] \cos^2 \theta$$

In (12), $n = n(\theta)$, and this and all other explicit functions of θ are to be considered implicit functions of γ through (6a). All notation not defined above is defined in other papers.⁴⁻⁸

With the aid of the foregoing formulation it is now possible to plot the mean radiated power pattern for electric and magnetic dipoles with arbitrary orientation in a cold collisionless magnetoplasma, for frequencies between the proton and electron gyrofrequencies. The radiation patterns so obtained have at least three outstanding characteristics:

1. The pattern is practically independent of the dipole orientation.
2. For frequencies f above the lower-hybrid-resonance frequency f_{LHR} and below the electron gyrofrequency, f_{He} , the radiated energy is confined entirely inside a cone about the static magnetic field line direction and no power is radiated directly across the field lines.
3. For f between the proton gyrofrequency, f_{Hp} , and $1/2 f_{He}$, most of the power flows in narrow major lobes which number between one and four.

In all cases the major lobes of the pattern are found to be due to focusing effects which result either from the presence of inflection points on the whistler mode refractive index surface or from the presence of minima in the quantity $n(\theta)\cos\theta$ for $\theta \neq 0$. Focusing from the latter factor was neglected by the authors of a recent paper in the field.⁸

Figure 1 shows some representative normalized radiation patterns for the case in which it is assumed that the ratio of plasma frequency to electron gyrofrequency, f_p/f_{He} , is equal to 5, that the distance between source and observation point is equal to 500 km, and that the plasma consists of equal numbers of electrons and protons. The individual plots were chosen to show the typical transitions in the power pattern that occur as f varies from f_{He} to f_{Hp} . The plots are shown only for the positive x direction, but the plots for the negative x direction can be obtained through a reflection through the origin. Figure 1a shows the normalized power pattern for a small loop antenna for $f/f_{He} = 0.75$ and for two values of φ , 0 and $\pi/2$. Since $f > 1/2 f_{He}$, no focusing effects occur and no major lobes exist. The enhancement of radiation near the confinement cone is not a true lobe. Figure 1b is plotted for $f = 0.25 f_{He}$ and shows the pattern for both a small dipole (D) and a small loop (L). For this case the patterns are essentially independent of φ . For this f focusing effects occur and three major lobes appear, two due to inflection points on $n(\theta)$ and one due to a minima in $n(\theta)\cos\theta$. Figure 1c is plotted for $f = 7 \times 10^{-3} f_{He}$ and four major lobes appear, all due to first order inflection points on $n(\theta)$. Figure 1d is plotted for a value of f at which the first order inflection points of $n(\theta)$ merge to become higher order inflection points. In this case only two major lobes exist. Figure 1e is plotted for a value of f close to f_{Hp} at which no inflection points exist on $n(\theta)$. In this case no major lobes are seen in the pattern.

Plots such as shown in Figure 1 indicate that focusing effects should be of significant importance in the design of a VLF satellite transmitting system, especially one used in the study of wave-particle interactions in the magnetosphere.

References:

1. Kuehl, H. H., *Phys. Fluids*, **5**(9), pp. 1095-1103, 1962.
2. Arbol, E. and L. D. Felsen, *Electromagnetic Theory and Antennas*, Pt. 1, ed. E. C. Jordan, Pergamon Press, New York, pp. 421-459, 1963.
3. Staras, H., *IEEE Trans. on Ant. & Prop.*, **12**(6), pp. 695-702, 1964.
4. Wang, T.-N.C. and T. F. Bell, *Radio Sci.*, **4**(2), pp. 167-177, 1969.
5. Wang, T.-N.C. and T. F. Bell, *Radio Sci.*, **5**(3), pp. 605-610, 1970.
6. Bell, T. F. and T.-N.C. Wang (to be printed in July, issue of *IEEE Trans. On Ant. & Prop.*, 1971).
7. Wang, T.-N.C. and T. F. Bell, *IEEE Trans. On Ant. & Prop.*, **AP-17**(6), pp. 824-827, 1969.
8. Gia Russo, D.P. and J. S. Borgoson, *Radio Sci.*, **5**(4), pp. 745-756, 1970.

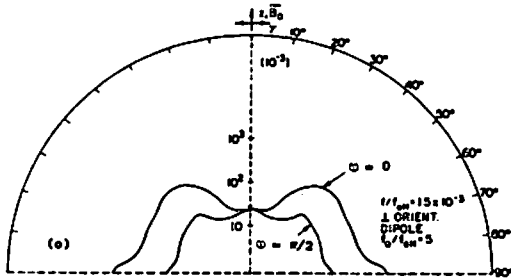
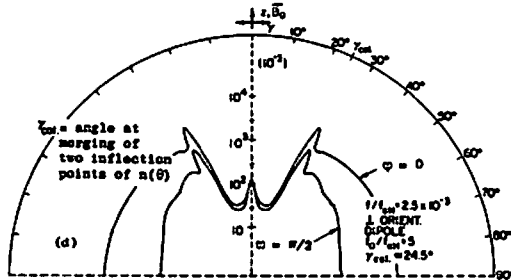
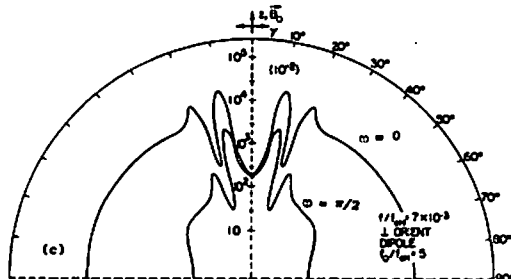
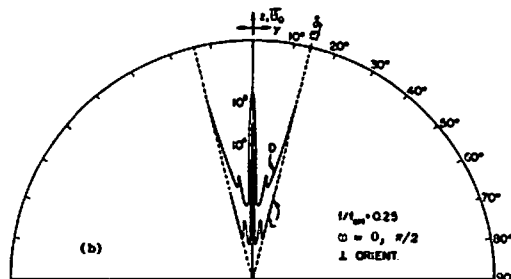
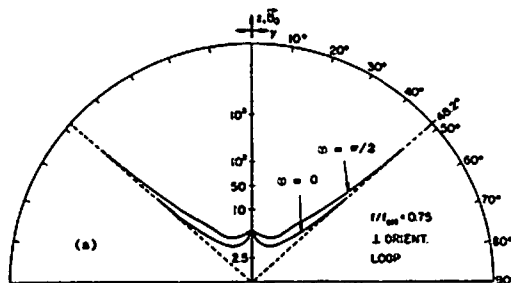


Figure 1. Representative normalized radiation patterns for small loops and dipoles, where the curves for the dipole are normalized with respect to C_d^2/f and those for the loop are normalized with respect to $C_L^2(f/f)^2$.